

Nondestructive characterization of microstructure and mechanical properties of intercritically annealed dual-phase steel by magnetic Barkhausen noise technique

S. Ghanei*, A. Saheb Alam, M. Kashefi, M. Mazinani

Department of Materials Engineering, Faculty of Engineering, Ferdowsi University of Mashhad, Mashhad, Iran

ARTICLE INFO

Article history:

Received 14 January 2014

Received in revised form

3 April 2014

Accepted 4 April 2014

Available online 13 April 2014

Keywords:

Barkhausen noise

Dual-phase steel

Martensite

Mechanical properties

Microstructure

Nondestructive evaluation

ABSTRACT

Detection of microstructural changes is a great importance matter in production line of steel parts. To implement such a task, many destructive tests are involved in industries. Current work examines the effects of different microstructures and mechanical properties on the magnetic Barkhausen noise technique as a suitable alternative testing method. In this study, different dual-phase steels with different martensite percentages were manufactured using various intercritical annealing temperatures from 750 to 850 °C. The results concerning magnetic Barkhausen noise were discussed in terms of position, height and shape of Barkhausen noise profiles, taking into account the effect of different percentages of martensite. Since this method is nondestructive after calibration, some beneficial relations for nondestructive characterization of microstructure as well as mechanical properties of any unknown dual-phase steel sample were achieved. Additionally, the feasibility of using the magnetic Barkhausen noise to detect microstructural changes during tempering of dual-phase steels was evaluated. The results revealed this magnetic method had a high potential to be used as a reliable nondestructive tool to detect microstructural changes occurring during manufacturing of dual-phase steels.

© 2014 Elsevier B.V. All rights reserved.

1. Introduction

The main feature in the selection of engineering materials, for using in industries, is the combination of performance and ultimate price. In this regard, there has been a growing attention in the manufacturing of dual-phase (hereafter denoted as DP) steels. DP steels are characterized by combination of special mechanical properties such as continuous yielding behavior, low yield strength, high tensile strength (due to their rapid work hardening rate), and good formability [1,2]. Combination of these desirable properties are derived from the composite type microstructure of the DP steels in which, soft ferrite matrix transfers the load to the martensite as the reinforcing phase [3,4].

Due to the composite type microstructure of the DP steels, ferrite and martensite constrain each other during deformation [5], as Kim and Thomas [6] reported that martensite phase constrains the deformation of ferrite around itself. Consequently, mechanical properties of the DP steels have a strong dependence on the martensite phase percentage. The higher percentage of martensite causes an increase in the yield and ultimate tensile strengths of

the DP steels [7–9], and on the counter, a decrease in the total elongation of them [6,8].

Conventional characterization methods of microstructure and mechanical properties of the DP steels are destructive tests, which are expensive and also time consuming. Another useful technique that can be used is nondestructive tests. In this connection, the present study tries to examine a magnetic nondestructive method, called magnetic Barkhausen noise (MBN), for characterization of microstructure and mechanical properties of the DP steel. The MBN is one of the micromagnetic techniques, which have been considered as a potential nondestructive testing technique for microstructural characterization of ferromagnetic materials under various conditions including fatigue, irradiation, stress, and heat treatment [10].

Principles of the MBN technique can be summarized as follows [11–13]. In the process of magnetization of the ferromagnetic sample (as a time varying magnetic field increases), the nucleation, the motion and the annihilation of magnetic domain walls occurs which result in the nucleation and growth of magnetic domains. During the motion of the domain wall for growth of domain, the barriers (precipitates, grain boundaries, inclusions, dislocation pile-ups, etc) in their path can pin them and leads in their discontinuous motions. Discontinuous movement of the domain wall is responsible for the production of a pulsating

* Corresponding author. Tel./fax: +98 5118763305.

E-mail address: Sadegh.Ghanei@yahoo.com (S. Ghanei).

magnetization (a noise like signal) corresponding to the changes of magnetic flux. This phenomenon which is due to the irreversible movement of magnetic domain walls, called the Barkhausen effect, induces a noise in the pick-up coil placed near the testing material in the form of voltage pulses.

A typical utilization of the MBN includes extracting of certain features from the measured signal and comparison of this information to the studied material properties. Typical calculated features are the root-mean-square (RMS) [14] and the MBN energy [15] and a more recent approach considers the peak height, position and width of the MBN profiles [16].

The MBN technique has received increasing attention for applying to on-line inspection in manufacturing industries such as automotive, aerospace and metallurgical machinery [17]. The MBN was reported to be useful for nondestructive evaluation of both micro- and macro-residual stresses [18], detection of deleterious phase [11] and different pearlite percentages [12], investigation of different grain sizes [19], identification of different stages of the tensile deformation [10,20], and monitoring of fatigue damages [21].

An attempt was made in the current study to investigate the effect of different DP microstructures on the MBN measurements in order to explore the possibility of using this method for verifying the intercritical annealing heat treatment results. Observations of the MBN method were correlated with mechanical characterization and metallographic examination. It was the aim of this technique to find some beneficial relations for nondestructive characterization of microstructure as well as mechanical properties of any unknown DP steel sample, since this method is quasi-instantaneous and nondestructive after calibration. Furthermore, as this method is sensitive to the microstructural changes, the feasibility of using the MBN sensor to detect changes during tempering of the DP steels was evaluated.

2. Experimental procedure

2.1. Materials and processing

The starting material investigated in this study was cold rolled low carbon steel with an initial microstructure of mainly ferrite with small amount of banded pearlite. The chemical composition of the investigated steel was Fe–0.08C–0.41Mn–0.50Si–0.09P–0.23Ni–0.39Cr–0.32Cu (wt%). The steel sheets (1.3 mm thick) were cut with the dimensions of 200 mm × 20 mm.

Several procedures were used here to produce final DP steels. First, in order to eliminate the effect of rolling, prepared specimens were normalized in γ region at 950 °C for 20 min. Afterwards, normalized steels were held in the various intercritical annealing temperatures between A_{C1} and A_{C3} (750, 765, 782, 810, 820, 832 and 850 °C for 15 min) in order to produce DP samples with different volume fraction of martensite phase and finally, all specimens were quenched into a 10 wt% brine solution held at –1 °C.

Although DP steels are usually used in as-quenched condition in order to take the advantage of the strengthening effect of hard martensite, for those industrial applications in which they may be heated to high temperature as in galvanizing treatment [22], the tempering of martensite may be an issue. Since the mechanical behavior of the DP steels depend mainly on martensite, one may expect that the mechanical behavior of the DP steels changes with tempering. To investigate this issue, in a selected case, samples were tempered at 200 °C and 300 °C for 60 min.

Metallographic samples were prepared from heat treated specimens and metallographic sections of these specimens were mechanically polished using successive polishing steps (600, 1200

and 2000 grit papers and 0.1 μm alumina slurry). Polished surface of specimens were etched in a solution obtained by dissolving 10 g sodium metabisulfite ($\text{Na}_2\text{S}_2\text{O}_5$) in 100 mL distilled water. The mentioned solution produces a strong contrast between the white ferrite and the dark regions of martensite which is suitable for phase percentage measurements. Up to 25 optical microscopic images from different locations in each DP sample were taken and after that, microstructural analysis was performed and martensite percentage in each sample was calculated using Clemex image analyzer.

According to ASTM E8M standard, flat tensile specimens of 50 mm gauge length and 12.5 mm gage width were prepared. Tensile tests were conducted using a Zwick/Z250 testing machine at a strain rate of 0.002 s^{-1} and stress–strain plots were obtained in each case. It has to be added that, three tensile specimens were tested for every condition.

Additionally, Vickers's hardness tests were carried out at 10 kg load for 30 s, according to ASTM E384 standard. An average of at least 10 hardness measurements has been reported for each specimen.

2.2. Nondestructive evaluation

In order to measure and evaluate the MBN signals, the tests were carried out using the experimental system designed and developed in the authors' laboratory. Fig. 1 shows schematic illustration of the device used in this study consisting of a sinusoidal shaped current generator with a wide range of frequencies (0.5 Hz–5 MHz), the amplifiers, a probe (consisting of excitation and pick-up coils) and an A/D converter. Design of the probe was done with respect to the sample's shape. The excitation magnetic field is provided using a U-shape ferritic core with a 500 turns of 0.35 mm insulated copper wire coil around it. This equipment keeps the sheet specimens near magnetic saturation. To minimize undesirable effect of eddy currents in induction process, a relatively low excitation frequency was used. In order to ensure the perfect reproducibility of the measurements, a fixed rate of magnetization was imposed to the DP specimens. Detection of the MBN signals was carried out through a pick-up coil, placed at the surface of the test material between the poles of U-shape coil, with 750 turns of 0.15 mm insulated copper wire, which was wound on a cylindrical ferritic core. Detected MBN signals were amplified, band pass filtered (3–200 kHz) and re-amplified. Then, the MBN signals were digitized and monitored using a digital oscilloscope (the A/D card) and eventually, were sent to a PC for processing. The MBN signals are usually packaged into an envelope profile which is provided using the root-mean-square (RMS) of the MBN signals as a function of time/magnetizing field.

Frequency determination is the first step for the MBN measurements. There are two methods for determining the optimum frequency: 1 – using the equation of electromagnetic skin depth, 2 – applying regression analysis between material properties and the MBN outputs.

First way for determination of optimum frequency for the MBN measurements [23] uses the equation of electromagnetic skin depth (δ), where the magnetic field drops to 37% of its maximum

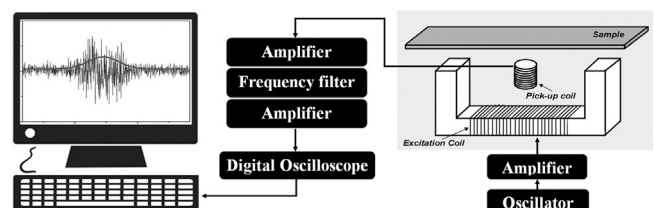


Fig. 1. Schematic illustration of the MBN circuit.

value, expressed as

$$\delta_{(f,\mu,\sigma)} = \frac{1}{\sqrt{\pi f \mu \sigma}} \quad (1)$$

where f is the frequency, σ is the conductivity and μ is the permeability.

The first method is preferred in some situations, for example, to determine the decarburizing depth [24]. It should be noted that, applying this method is not possible here due to the different values of conductivity and permeability for the DP samples with different percentages of martensite. For a fixed depth, the frequency is a function of the conductivity and the permeability of the material. Accordingly, this method cannot provide a fixed frequency for a fixed depth, so it was not considered here.

In order to determine the optimum frequency by the second method, preliminary measurements on the MBN outputs were made over a range of frequencies from 1 to 11 Hz (in 1 Hz steps). This range was used to minimize the undesirable effect of eddy currents to the applied magnetic field and to ensure a relatively fix rate of magnetization in the DP specimens [25]. Furthermore, low frequencies can gather enough information from volume of the investigated steels at greater depths instead of near surface magnetization [23]. The optimum frequency has been determined by applying regression analysis and choosing a frequency with the best relations between different MBN outputs and materials properties. According to the results, frequency of 7 Hz was chosen as the optimum frequency due to the highest correlation coefficient value.

To investigate the obtained MBN signals and their relationship with mechanical properties as well as the microstructure of the DP samples, the parameters of position and height of the MBN peaks were used. In each case, 10 signals were averaged and the background noise was removed.

3. Results and discussion

3.1. Microstructure and mechanical properties

Fig. 2 shows the DP microstructure of intercritically annealed specimen developed by heat treatment for 15 min at 810 °C, and then quenched in an iced brine solution to obtain 37% of martensite phase. Dark and bright regions represent the martensite and the ferrite, respectively.

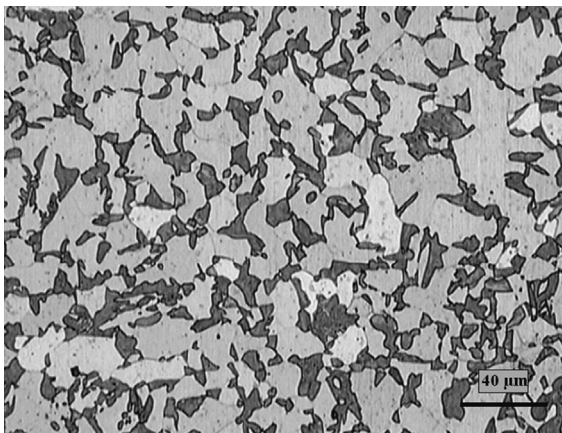


Fig. 2. Optical microscopic image of the DP microstructure intercritically annealed for 15 min at 810 °C to obtain 37% of martensite phase which etched in sodium metabisulfite solution (dark and bright regions represent the martensite and the ferrite, respectively).

Metallographic images of the as-received steel clearly exhibited banding due to the rolling. In order to eliminate the effect of rolling in final steels, especially in tensile test specimens, primary normalization heat treatment in γ region was performed. Because of this heat treatment, all manufactured DP steel specimens did not show any signs of banding and martensite islands had a globular morphology that was finely dispersed (see Fig. 2). As a result, DP specimens had no anisotropy.

Different DP steels of the present work were produced with various intercritical annealing temperatures. According to Table 1, an increase in the intercritical annealing temperature caused an increase in the martensite phase percentage. As a result of setting an elevated annealing temperature, higher amount of austenite formed in the area of intercritical heating and in consequence of that, higher martensite phase appeared in the resulted DP microstructure, having lever rule in mind.

Mechanical properties of the DP steels are tabulated in Table 1. The higher intercritical annealing temperature led to the steels with an improvement in both yield and ultimate tensile strengths, whereas the total elongation of them decreased which were consistent with the findings of previous researches [6,9].

Due to the presence of hard second phase of martensite within the ferritic matrix, yield point phenomenon does not observe in the tensile stress–strain curves of the as-quenched DP steels [1,26]. Abundant of unpinned dislocations generated in ferritic matrix as a result of plastic deformation during martensite transformation, and the movement of these dislocations is responsible for the absence of yield point [27,28]. As can be clearly seen in the tensile stress–strain curves of the as-quenched DP specimens of the present investigation in the Fig. 3, no yield point phenomenon was observed, suggesting successful productions of the composite type microstructure of the DP steels by intercritical annealing processes. It should be added that to achieve a continuous yielding behavior, at least 4% of martensite in DP steels is necessary [8].

The stress–strain curves of the sample D-45, before and after tempering at different temperatures are shown in Fig. 4. As can be seen in the figure, the as-quenched sample has a smooth stress–strain curve, but the yield point phenomenon was returned to some extent at two tempering temperatures. At tempered samples, the content of interstitial atoms in intergrains is deficient for pinning of dislocations, but long range diffusion of these atoms from interior parts of the grains compensates the lack of them, which leads to return of discontinuous yielding behavior [22]. Although ultimate tensile strength (UTS) value of DP steel decreased from 743 to 612 MPa after keeping the sample at the aforementioned tempering heat treatment, total elongation value of the investigated steel increased from 7.65% to 9.71% which is consistent with the results from the literature [22,29–32]. However, in the present study, there is no obvious trend for the result of yield strength as other related investigations, which unanimous agreement on the conclusion of yield strength dependence of different tempering temperatures has not been reached. For example, Sayed and Kheirandish [22] and Hayashi et al. [32] reported an increase in the yield strength after tempering at low temperatures, while, a decrease for higher tempering temperatures. Gündüz [31] observed no significant variation in yield strength of the DP steel at different tempering temperatures. Also, Tavares et al. [29] concluded that the yield stress decreased linearly with the tempering temperatures.

Vickers's hardness numbers (VHN) of the DP steels are listed in Table 1. The obtained results show that an increase in the martensite percentage results in an increase in the hardness of DP steel samples from D-17 to D-58. Also, at tempered samples, martensite became softer and more ductile through which an increase in the tempering temperature resulted in a decrease in the VHN values.

Table 1
Heat Treatment cycles for producing different microstructures and the corresponding results of the experiments.

Specimen name	D-17	D-23	D-28	D-37	D-40	D-45	D-58	D-45-T200	D-45-T300
Intercritical temperature (°C)	750	765	782	810	820	832	850	832	832
Tempering condition	–	–	–	–	–	–	–	200 °C-60 min	300 °C-60 min
Martensite percentage (%)	17	23	28	37	40	45	58	45	45
Hardness (Vickers)	205	215	229	251	257	259	267	245	238
Yield strength (MPa)	398	400	405	433	440	466	482	335	403
Ultimate tensile strength (MPa)	660	676	680	690	720	743	756	620	612
Elongation (%)	9.92	9.86	9.90	7.95	7.90	7.65	7.47	9.40	9.71

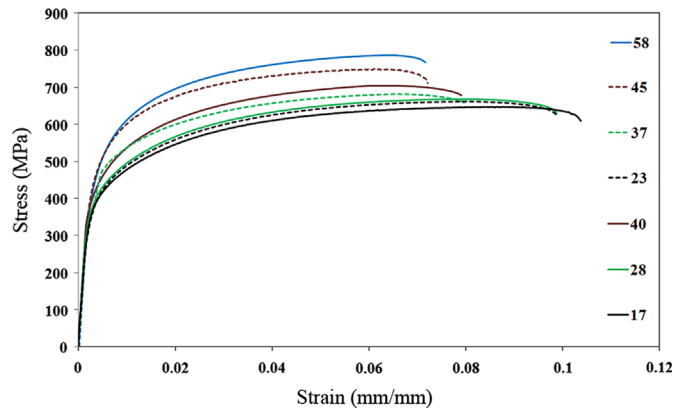


Fig. 3. Stress–strain curves of the as-quenched DP steels with different percentage of martensite.

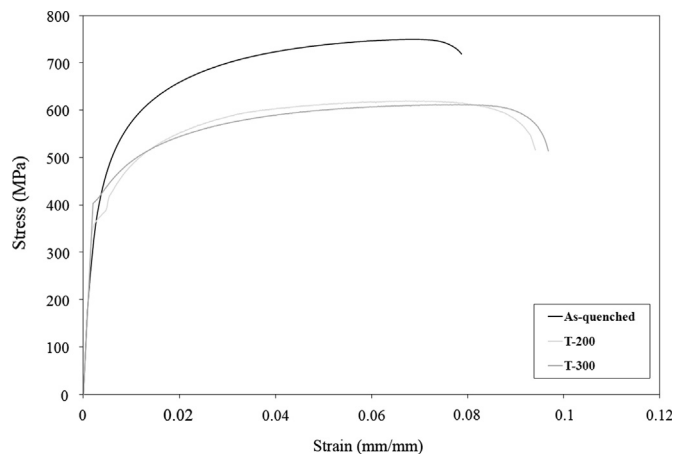


Fig. 4. The stress–strain curves of the sample D-45, before, and after tempering at 200 °C and 300 °C.

3.2. MBN measurements

Fig. 5 shows the evaluation of the mechanical properties of the DP steels as a function of the MBN peak characteristics, i.e. height and position. As can be seen in the figure, the values of the peak height/position increased with the increase in the hardness, yield and ultimate tensile strengths of the investigated DP steels. Using simple regression analysis, second degree polynomial fit was found to be the best for the analysis of the collected data. In order to study the discrepancy between experimental data and polynomial fits, correlation coefficients (R^2) were introduced. For the relationships shown in Fig. 5, the amount of correlation coefficients are very high ($0.9411 < R^2 < 0.9822$) and this high accuracy can help to separate the DP steel samples based on their mechanical properties. Implementing this hand probe for prediction of mechanical properties with a good accuracy, it is only necessary to non-destructively evaluate of any unknown DP steel sample by the

MBN device and put the obtained value of peak height/position into the obtained quadratic equation for each polynomial fit of Fig. 5.

Microstructural changes influence the mechanical properties. These changes also affect the magnetic properties of the materials and corresponding MBN signals [33]. The obtained results of Fig. 5 show the indirect relationship between the magnetic and mechanical properties of the DP steel samples in which this results reveal the effect of microstructure on them. Then, it is useful to investigate the effect of microstructure here. The effect of different martensite percentages on the MBN profiles of the DP steel is shown in Fig. 6. It can be seen in the MBN profiles that an increase in the martensite percentage results in an increase in the peak height which is characteristic of the existence of the higher magnetically hard martensite [25] in the DP microstructure. The DP sample with the lowest martensite percentage (D-17) shows the smallest peak size at a position close to the lower magnetic field which is characteristic of the existence of higher amounts of magnetically soft ferrite [13] in the DP microstructure.

For a more detailed study, peak height/position of the MBN profiles of the Fig. 6 were derived and plotted versus the martensite percentage of the DP steels, separately (Fig. 7). For characterization of these relations, moreover, second degree polynomial fit was chosen as the best fit for both graphs. Fig. 7 can be used as a tool for martensite percentage determination of any unknown DP steel sample due to the obtained quadratic equation for each polynomial fit with corresponding high correlation coefficient ($R^2 > 0.9619$). As in the cases of mechanical properties, slope of polynomial fits are positive, which shows an increase in the values of peak height/position with an increase in the martensite percentage of the DP steels.

The Barkhausen signal (V_{BN}) which is induced by the irreversible unpinning of domain wall, as the field increases, is given by [19]:

$$V_{BN} = NA\mu_0 n(H) \frac{dM}{dt} \quad (2)$$

where N , A , μ_0 and dM/dt are, the coil turns, the cross section area of the coil, the magnetic permeability of vacuum and the rate of changes in magnetization, respectively. In addition, $n(H)$ is the number of unpinning events which in general is a function of magnetizing field.

Number of pinning sites and corresponding unpinning events increased as the martensite phase in the microstructure of the DP steels increased, therefore according to the Eq. (2), resulted in an increase in the MBN signals. Both ferrite and martensite phases, due to the composite type microstructure of the DP steels, were contributing independently to the MBN signal according to their respective volume fractions. Although the ferrite and martensite were both ferromagnetic materials but ferrite phase in the DP steels was strongly ferromagnetic and had much higher magnetization than the martensite [34] which significantly affected the MBN measurements. Therefore, the effect of ferrite phase is considered here, primarily.

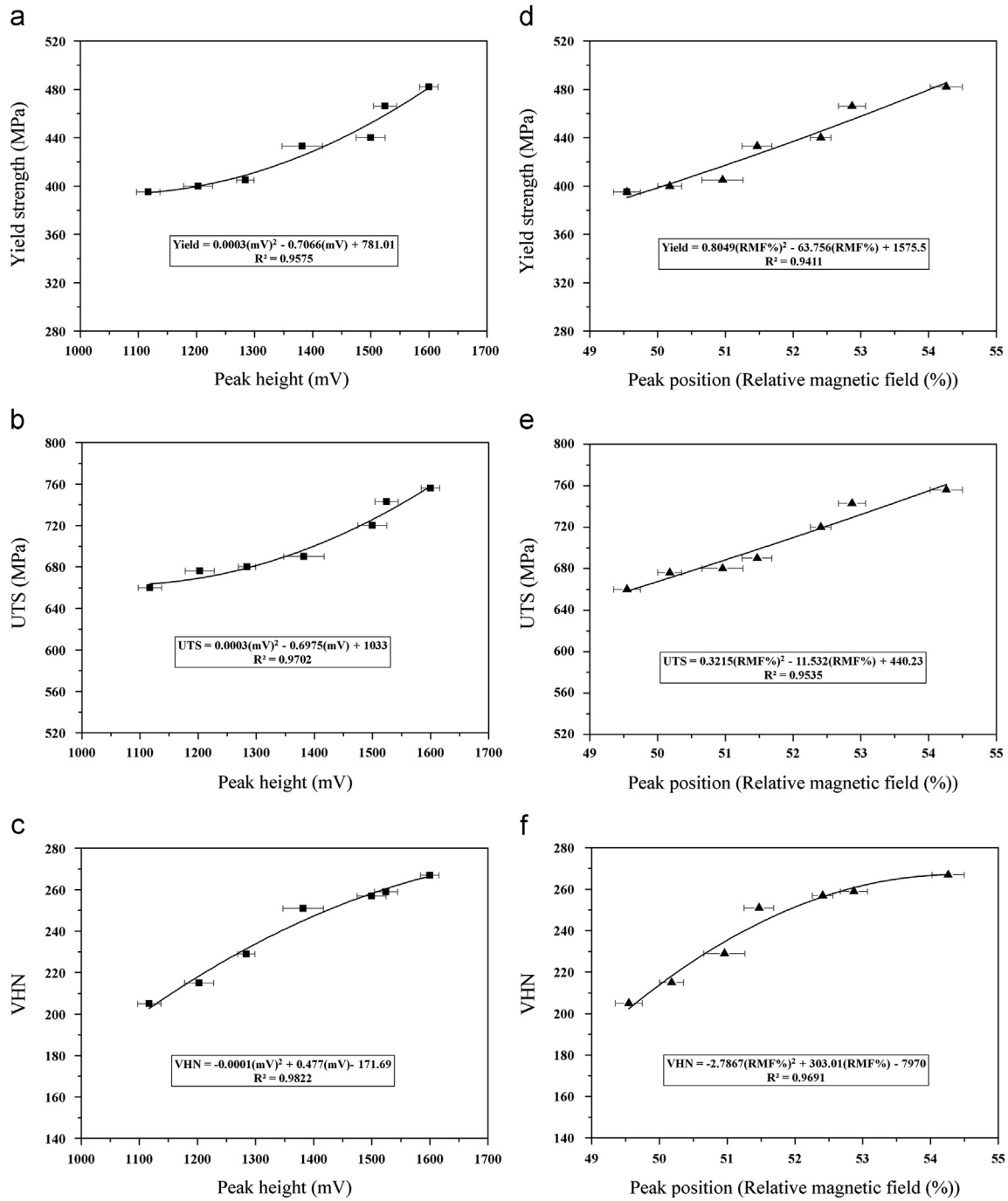


Fig. 5. Mechanical properties of the DP steels with different percentage of martensite as a function of the MBN peak characteristics. Relations of the MBN profiles' peak height and (a) yield strength, (b) UTS and (c) hardness, and relations of the MBN peak position and (d) yield strength, (e) UTS and (f) hardness.

A research into the effect of water quenching process on the hysteresis curves of the DP steels was done by Gao et al. [34], where they introduced the dislocation density and internal stress as the domain wall pinning reasons and they reported corresponding magnetic hardening with an increase in the martensite percentage. Hysteresis study and the MBN are both micromagnetic techniques which depend on domain wall movements [10], this means increasing the dislocation density and internal stress due to the increasing of the martensite percentage, were the main reasons for increasing the MBN signals, in the present study.

The presence of martensite can affect the ferrite phase by introducing additional dislocations in the ferrite structure in the

vicinity of martensite islands as a result of the plastic strain associated with the martensite transformation [27]. The density of additional dislocations introduced into the ferrite structure increases with increasing the martensite percentage.

On the other hand, martensite has a lower density than austenite, so that the martensitic transformation results to the volume expansion which leads to the increase in the internal stresses in ferrite phase.

Therefore, as the martensite percentage increased, the internal stresses and the dislocations density were also increased. Consequently, dislocation entanglement due to an increase in dislocation density occurred, which form more strong pinning sites in the path of domain walls.

In spite of magnetically hard nature of martensite, as a constituent of the composite type microstructure of the DP steels, it contributed independently to the MBN signal corresponding to its volume fraction. Martensite is formed in carbon steels by quenching of austenite that carbon atoms do not have time to diffuse out of the crystal structure. As a result, the FCC austenite transforms to a highly strained BCT form of ferrite that is super-saturated with carbon. This highly strained structure produced more pinning sites in the path of domain walls. Also, high density of crystal boundaries of martensite plates and the internal twins within the plates acted as effective barriers to domain wall motion [25]. Thus, an increase in martensite volume fraction resulted to an increase in the MBN signal.

In the experiments, peak position shifted to higher values of magnetic field as the martensite percentage in the DP microstructure increased (Fig. 6). As mentioned, an increase in the martensite percentage produced more strong pinning sites against propagation of domain walls, and so, larger field was required for their motion. According to the relationship between the MBN and hysteresis study [12,25], in Fig. 8, the observed broadening of the BH loop with this kind of DP microstructure [34] is consistent with the obtained results of the present study. An increase in the martensite phase resulted in the broadening of the BH loop of the DP steels which led to shift the point of coercive force away from the vertical axis (flux density axis). The amplitude of the MBN is greatest when the slope of the BH curve is maximum (at the point of coercive force). Accordingly, an increase in martensite phase in the DP microstructure led to shift the location of occurrence of the MBN peak to the higher values of magnetic field.

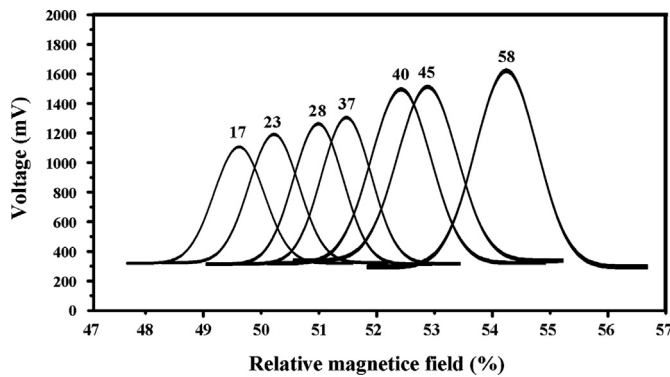


Fig. 6. The MBN profiles for different DP microstructures with different martensite percentages.

It is worth to note that, the single-peak MBN behavior, shown in the Fig. 6, occurs when the microstructure is dominated by high dislocation density [10]. The most important conclusion from this result is the great contribution of ferrite phase in magnetization

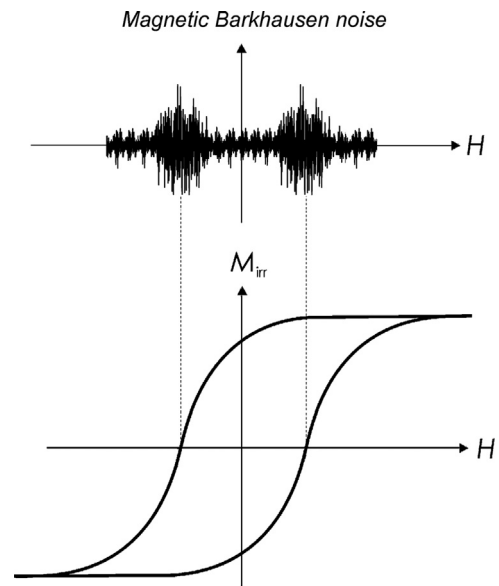


Fig. 8. Schematic illustration of the theoretical relation between the magnetization hysteresis loop and the MBN.

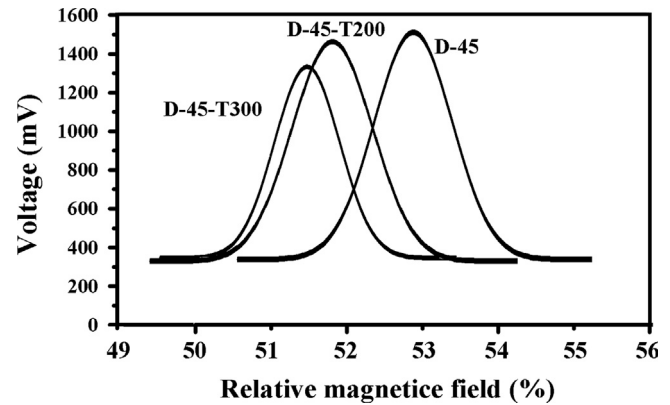


Fig. 9. The MBN profiles for the sample D-45, before and after tempering at 200 °C and 300 °C.

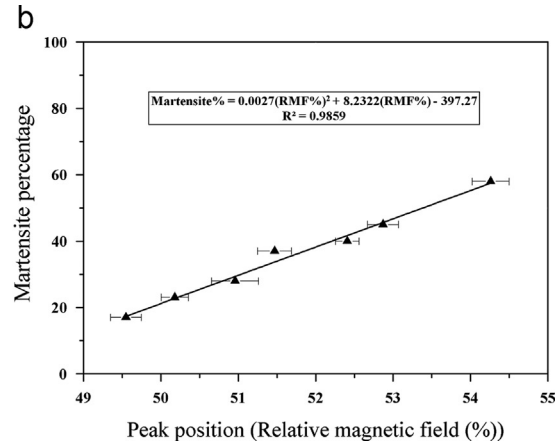
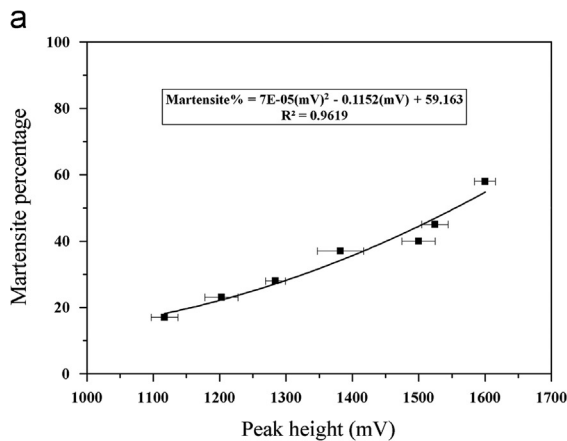


Fig. 7. Martensite percentage versus the MBN peak (a) height and (b) position.

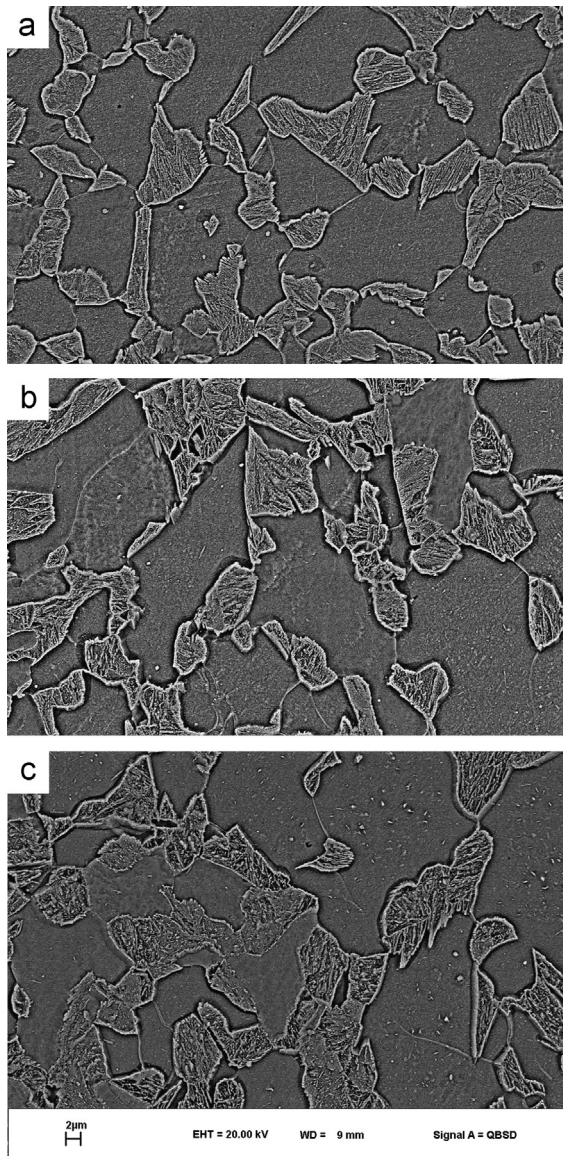


Fig. 10. (a) SEM micrograph of as-quenched specimens (intercritical annealing temperature: 832 °C; holding time: 15 min), (b) SEM micrograph of specimens tempered for 60 min at 200 °C, (c) SEM micrograph of specimens tempered for 60 min at 300 °C.

and reveals the high proportion of its dislocation density in production of the MBN.

Fig. 9 shows the differences in the MBN signal between the as-quenched and the tempered DP steel samples. The as-quenched DP microstructure had much effective barriers against domain wall motion due to the high dislocation density and internal stress in the ferrite phase as well as highly strained BCT structure of martensite, and in addition, high density of crystal boundaries of martensite plates and the internal twins within the plates. That is why the peak height of the as-quenched microstructures is higher than the tempered ones. Comparison of the microstructure of the as-received sample with the sample tempered at 200 °C did not show considerable difference (Fig. 10). At this condition, recovery of the defect structure in the martensite phase and the relief of the residual stresses in ferrite by the volume contraction of the martensite, are main parts of the tempering process [22,31]. Due to these, there are less effective barriers against domain wall motion in comparison with the as-quenched specimen. So, according to Eq. (2), the MBN peak height decreased. When the

tempering temperature was increased to 300 °C, ϵ -iron carbides started to precipitate and the martensite becomes less tetragonal, meanwhile the residual stresses further decreased [22,31]. As a result, the MBN peak height of the sample tempered at 300 °C further decreased.

Comparing profiles of the Fig. 9, one can readily observe that peak position shifted to lower values of magnetic field as the tempering temperature increased. As mentioned, an increase in the tempering temperature lessened the pinning sites against propagation of domain walls and so, a considerably less field is required for their motion.

4. Conclusions

MBN was successfully used for nondestructive characterization of microstructure and mechanical properties of the DP steel. It was found that, increasing the percentage of martensite resulted in the more pinning sites against the paths of domain walls and a corresponding increase in the MBN signals. High dislocation density and internal stresses in the ferrite structure as well as the high strain field of BCT, high density of crystal boundaries of martensite plates and the internal twins within the plates in the martensite phase were suggested as the strong barriers against the movements of domain walls which resulted in production of MBN signals. It was also observed that the MBN peaks of the DP steels tended to shift to the higher magnetic field as the martensite in the DP microstructure increased due to the larger field required for the motion of domain walls at the presences of the more pinning sites. It had also been demonstrated that the single-peak MBN behavior of the investigated steels is related to the high dislocation density. Using the indirect relationship between the mechanical and magnetic properties of the DP steels, enable us to develop a fast way for nondestructive prediction of mechanical properties of the DP steels by the MBN method. Recovery of the defect structure in the martensite phase, the relief of the residual stresses in ferrite, ϵ -iron carbides precipitation into the dislocations of the ferrite phase, and the reduction in tetragonality of martensite were the main microstructural changes during tempering of the DP steels. Such microstructural changes led to the less effective barriers against the movements of domain walls and corresponding decrease in the value of peak height/position of the MBN profiles.

References

- [1] M. Calcagnotto, D. Ponge, D. Raabe, *Mater. Sci. Eng. A* 527 (2010) 7832–7840.
- [2] J. Kadkhodapour, A. Butz, S. Ziaei Rad, *Acta Mater.* 59 (2011) 2575–2588.
- [3] W. Woo, V.T. Em, E.Y. Kim, S.H. Han, Y.S. Han, S.H. Choi, *Acta Mater.* 60 (2012) 6972–6981.
- [4] S. Ghanei, M. Kashefi, M. Mazinani, *Mater. Des.* 50 (2013) 491–496.
- [5] H. Lee, B. Hwang, S. Lee, C. Lee, S.-J. Kim, *Metall. Mater. Trans. A* 35 (2004) 2371–2382.
- [6] N. Kim, G. Thomas, *Metall. Mater. Trans. A* 12 (1981) 483–489.
- [7] K. Park, M. Nishiyama, N. Nakada, T. Tsuchiyama, S. Takaki, *Mater. Sci. Eng. A* 604 (2014) 135–141.
- [8] M. Asadi, B.C.D. Cooman, H. Palkowski, *Mater. Sci. Eng. A* 538 (2012) 42–52.
- [9] A. Bag, K. Ray, E. Dwarakadasa, *Metall. Mater. Trans. A* 30 (1999) 1193–1202.
- [10] V. Moorthy, S. Vaidyanathan, T. Jayakumar, B. Raj, B.P. Kashyap, *Acta Mater.* 47 (1999) 1869–1878.
- [11] P.G. Normando, E.P. Moura, J.A. Souza, S.S.M. Tavares, L.R. Padovese, *Mater. Sci. Eng. A* 527 (2010) 2886–2891.
- [12] L. Clapham, C. Jagadish, D.L. Atherton, *Acta Metall. Mater.* 39 (1991) 1555–1562.
- [13] K.M. Koo, M.Y. Yau, D.H.L. Ng, C.C.H. Lo, *Mater. Sci. Eng. A* 351 (2003) 310–315.
- [14] S. Santa-aho, M. Vippola, T. Saarinen, M. Isakov, A. Sorsa, M. Lindgren, K. Leiviskä, T. Lepistö, *J. Mater. Sci.* 47 (2012) 6420–6428.
- [15] C.G. Stefanita, D.L. Atherton, L. Clapham, *Acta Mater.* 48 (2000) 3545–3551.
- [16] A. Sorsa, K. Leiviskä, S. Santa-aho, T. Lepistö, *NDT & E Int.* 46 (2012) 100–106.
- [17] P. Wang, L. Zhu, Q. Zhu, X. Ji, H. Wang, G. Tian, E. Yao, *NDT & E Int.* 55 (2013) 9–14.
- [18] J.C. Sanchez, M.F. de Campos, L.R. Padovese, *J. Magn. Magn. Mater.* 324 (2012) 11–14.

- [19] D.H.L. Ng, K.S. Cho, M.L. Wong, S.L.I. Chan, X.Y. Ma, C.C.H. Lo, *Mater. Sci. Eng. A* 358 (2003) 186–198.
- [20] V.E. Iordache, E. Hug, N. Buiron, *Mater. Sci. Eng. A* 359 (2003) 62–74.
- [21] M. Lindgren, T. Lepistö, *NDT & E Int.* 33 (2000) 423–428.
- [22] A.A. Sayed, S. Kheirandish, *Mater. Sci. Eng. A* 532 (2012) 21–25.
- [23] V. Moorthy, B.A. Shaw, J.T. Evans, *NDT & E Int.* 36 (2003) 43–49.
- [24] S. Kahrobaee, M. Kashefi, A. Saheb Alam, *Surf. Coat. Technol.* 205 (2011) 4083–4088.
- [25] M. Blaow, J.T. Evans, B.A. Shaw, *Acta Mater.* 53 (2005) 279–287.
- [26] L.R. Bhagavathi, G.P. Chaudhari, S.K. Nath, *Mater. Des.* 32 (2011) 433–440.
- [27] E. Ahmad, T. Manzoor, N. Hussain, *Mater. Sci. Eng. A* 508 (2009) 259–265.
- [28] P. Movahed, S. Kolahgar, S.P.H. Marashi, M. Pouranvari, N. Parvin, *Mater. Sci. Eng. A* 518 (2009) 1–6.
- [29] S.S.M. Tavares, P.D. Pedroza, J.R. Teodósio, T. Gurova, *Scr. Mater.* 40 (1999) 887–892.
- [30] A. Kamp, S. Celotto, D.N. Hanlon, *Mater. Sci. Eng. A* 538 (2012) 35–41.
- [31] S. Gündüz, *Mater. Lett.* 63 (2009) 2381–2383.
- [32] K. Hayashi, K. Miyata, F. Katsuki, T. Ishimoto, T. Nakano, J. *Alloys Compd.* 577 (2013) S593–S596.
- [33] A. Bükki-Deme, I.A. Szabó, C. Cserhádi, J. *Magn. Magn. Mater.* 322 (2010) 1748–1751.
- [34] L. Gao, Y.M. Zhou, J.L. Liu, X.D. Shen, Z.M. Ren, J. *Magn. Magn. Mater.* 322 (2010) 929–933.